Proc. Natl. Acad. Sci. USA
Vol. 93, pp. 11080–11084, October 1996
Medical Sciences

Independence of metastatic ability and extravasation: Metastatic *ras*-transformed and control fibroblasts extravasate equally well

(metastasis/invasion/*in vivo* videomicroscopy)

SAHADIA KOOP*, ERIC E. SCHMIDT*, IAN C. MACDONALD*, VINCENT L. MORRIS*†‡, RAMA KHOKHA‡§¶, MARSHA GRATTAN†, JAMES LEONE*, ANN F. CHAMBERS*†‡¶‖, AND ALAN C. GROOM*,**

Departments of *Medical Biophysics, †Microbiology and Immunology, ‡Oncology, and §Biochemistry, University of Western Ontario, London, ON Canada N6A 5C1; ¶London Regional Cancer Centre, London, ON Canada N6A 4L6; and **John P. Robarts Research Institute, London, ON Canada N6A 5K8

Communicated by George F. Vande Woude, Frederick Cancer Research and Development Center, Frederick, MD, July 11, 1996 (received for review April 18, 1996)

ABSTRACT **Escape of cancer cells from the circulation (extravasation) is thought to be a major rate-limiting step in metastasis, with few cells being able to extravasate. Furthermore, highly metastatic cells are believed to extravasate more readily than poorly metastatic cells. We assessed *in vivo* the extravasation ability of highly metastatic *ras*-transformed NIH 3T3 cells (PAP2) versus control nontumorigenic nontransformed NIH 3T3 cells and primary mouse embryo fibroblasts. Fluorescently labeled cells were injected intravenously into chicken embryo chorioallantoic membrane and analyzed by intravital videomicroscopy. The chorioallantoic membrane is an appropriate model for studying extravasation, since, at the embryonic stage used, the microvasculature exhibits a continuous basement membrane and adult permeability properties. The kinetics of extravasation were assessed by determining whether individual cells (n = 1481) were intravascular, extravascular, or in the process of extravasation, at 3, 6, and 24 h after injection. Contrary to expectations, our results showed that all three cell types extravasated with the same kinetics. By 24 h after injection >89% of observed cells had completed extravasation from the capillary plexus. After extravasation, individual fibroblasts of all cell types demonstrated preferential migration within the mesenchymal layer toward arterioles, not to venules or lymphatics. Thus in this model and for these cells, extravasation is independent of metastatic ability. This suggests that the ability to extravasate *in vivo* is not necessarily predictive of subsequent metastasis formation, and that postextravasation events may be key determinants in metastasis.**

Metastasis, the spread of cancer cells from a primary tumor to distant sites, is the major cause of death from cancer. Mortality results from the direct anatomical and physiological effects of metastases on other organ systems (e.g., brain and liver) or sometimes from complications associated with treatment (1, 2). The metastatic process is thought to include the following steps: detachment of cancer cells from the primary tumor, invasion of surrounding tissue, entrance into blood or lymphatic vessels (intravasation), transport to new sites, escape from the microvasculature (extravasation), invasion of target tissue, and growth of metastatic tumors (3–5). Cancer cells also must evade the immune system throughout the metastatic process.

Extravasation is thought to be a major rate-limiting step in metastasis, with only a few cancer cells capable of degrading the basement membrane and extracellular matrix to escape from microvessels. Moreover, poorly metastatic cells are believed to extravasate less readily than highly metastatic cells (4, 6–8). Our recent results from intravital videomicroscopy have raised questions about these views. Using *in vivo* assays with a variety of cell types (including melanoma and mammary carcinoma) in chicken embryo chorioallantoic membrane (CAM) and mouse liver, we found that the majority of observed cancer cells had extravasated within 24 h of intravenous injection and that cells with different metastatic abilities exhibited the same time course of extravasation (9–11). Moreover, when a "cell accounting" procedure was used to quantify the proportion of the total number of injected cells that had extravasated from the CAM microvasculature by 24 h after injection, we found this proportion to be >80% for melanoma cells of varying metastatic abilities (9). These findings suggested that the ability to extravasate can be independent of the metastatic potential and led us to question the general applicability of this phenomenon. Therefore, in the present study, we assessed the extravasation ability of highly metastatic H-*ras*-transformed NIH 3T3 cells (PAP2) versus nonmetastatic control NIH 3T3 cells, in the CAM. The CAM is an appropriate model for studying cell extravasation from the microcirculation since, at the embryonic stage used, the microvasculature has continuous endothelium and basement membrane and adult permeability properties (12–14). In an attempt to test cells that would not be expected to extravasate (and since NIH 3T3 cells are immortalized embryonic mouse fibroblasts), we also used a second control, primary fibroblasts cultured directly from mouse embryos (MEFs). While embryonic fibroblasts in general are very motile, the cells used in the present study have been shown to differ in their *in vivo* and *in vitro* properties. NIH 3T3 cells are poorly invasive *in vitro* and nontumorigenic and nonmetastatic in chicken embryo and mouse (15–18) and were predicted to have limited ability to extravasate. Similarly, MEFs were predicted to show little or no ability to extravasate. In contrast, PAP2 cells express high levels of H-*ras* oncogene, are invasive *in vitro*, and are tumorigenic and metastatic in chicken embryo and mouse (15–18). PAP2 cells were thus predicted to have the highest ability to extravasate.

MATERIALS AND METHODS

Cell Culture and Fluorescent Labeling Procedures. PAP2 cells (H-*ras*-transformed NIH 3T3 cells) and NIH 3T3 (nontransformed but immortalized murine fibroblasts) were maintained in tissue culture in Dulbecco's minimal essential medium (Life Technologies, Burlington, Ontario, Canada) plus 10% calf serum (Life Technologies), as described (15). These cells were grown for no more than 4–6 weeks in culture.

The publication costs of this article were defrayed in part by page charge payment. This article must therefore be hereby marked "*advertisement*" in accordance with 18 U.S.C. §1734 solely to indicate this fact.

Abbreviations: MEF, mouse embryo fibroblast; CAM, chorioallantoic membrane; p.i., post-injection.

‖To whom reprint requests should be addressed at: The London Regional Cancer Centre, 790 Commissioners Road East, London, ON, N6A 4L6, Canada. e-mail: annfc@julian.uwo.ca.

Primary mouse fibroblasts were cultured directly from 13- to 14-day-old embryos (NIH Swiss mice; Harlan–Sprague–Dawley). Single cell suspensions of fibroblasts were obtained by trypsinization (0.25% trypsin in phosphate-buffered saline minus Ca^{2+} and Mg^{2+}). The cells were removed from the trypsin solution by centrifugation (1000 × *g*), resuspended in α-minimal essential medium plus ribonucleosides (Life Technologies) with 10% fetal calf serum (HyClone), penicillin (100 units/ml), and streptomycin (100 μg/ml; Life Technologies), and plated in T150 flasks in an atmosphere of 5–7% CO_2. The cells were allowed to undergo no more than three passages before use and were harvested at subconfluence.

Cells were fluorescently labeled using Fluoresbrite carboxylate microspheres of 0.05- to 0.07-μm diameter (Polysciences) or Calcein-AM (Molecular Probes) as described (10, 19). Membrane integrity of the labeled cells was assessed before the experiments by adding a drop of ethidium bromide (0.01 mg/ml) to an equal volume of cell suspension on a coverslip. Cells were scored by fluorescence microscopy as either excluding ethidium bromide (green fluorescence) or as having taken it up (red fluorescence) as described (11). For all three cell types, >95% of the cells excluded ethidium bromide immediately before injection. The mean *in vitro* cell diameter was 17 μm for all cell types.

Intravital Videomicroscopy. We used intravital videomicroscopy of the CAM, the respiratory organ of the chicken embryo, which provides an immune-deficient model easily accessible for observation without the need for surgery (19). An immune-deficient host allows the study of steps in metastasis independent of host immune responses, modeling the clinical situation in which some cancer cells evade the immune system. Eggs containing 12-day-old embryos were removed briefly from the incubator and a small window was cut in the shell over a vein, leaving the CAM intact, as described (19, 20). Cells were injected into a CAM vein (10^6 cells per embryo in 0.1 ml of OptiMEM; Life Technologies); no damage was inflicted on the CAM during injection, as judged by lack of bleeding and intact appearance of the CAM vasculature by intravital videomicroscopy. The window was then resealed and the egg returned to the incubator pending further observation. At 3, 6, and 24 h postinjection (p.i.), the shell and outer shell membrane of individual eggs were removed from the air sac region (i.e., a different area than that used for cell injection). The inner shell membrane was rendered transparent with mineral oil to permit observation of intact CAM vessels and surrounding tissue. A lateral window on the shell allowed oblique transillumination via a fiber optic guide, providing high-contrast images. *In vivo* videomicroscopy was carried out using an epifluorescence inverted microscope (Diaphot TMD; Nikon), with the CAM positioned above the objective lenses (×10–×100). Episcopic illumination with fluorescence excitation wavelength 450–490 nm was used alone or superimposed on the image from transillumination. Images were viewed using a black and white video camera (model WV1550, Newvicon; Panasonic) and television monitor. A character generator added time, date, and stopwatch information to the video signal, and the combined signal was recorded on SVHS videotapes. In addition to the analysis at 3, 6, and 24 h p.i., we observed in real time the process of initial arrest of cells within the CAM microcirculation during injection, in several experiments.

By means of intravital videomicroscopy, one can clearly observe the arrangement of the CAM microcirculation and direction of blood flow in different vessel types, including views in the *z*-direction (above and below an initial plane of focus) obtained by "optical slicing" (for details see ref. 19). A rich capillary plexus lies directly beneath the inner shell membrane, exhibiting structural similarity with mammalian lungs (14, 21). This capillary plexus appears as a network of short, highly interconnected capillary segments, providing for almost a continuous sheet of blood except where tissue "posts" function as spacers (see figures 2 and 3 in ref. 19). The plexus is served by interdigitating arterioles and venules, seen by focusing on the mesenchymal layer just beneath. An extensive system of lymphatic vessels is also observed within the mesenchyme. Arterioles can easily be distinguished from venules based on their branching pattern together with the direction of blood flow. The flow is divergent in arteriolar branches, ultimately reaching the capillary plexus and draining into small venules, at which point the flow becomes convergent as venules join and lead into veins. Lymphatics are recognized by their thin endothelial walls and absence of blood flow, although infrequently individual red blood cells or leukocytes can be observed moving very slowly within these vessels.

At the time of the intravenous injections (12-day-old chicken embryo), the capillaries of the CAM have a continuous endothelial lining and a complete basement membrane, with permeability properties of mature vessels (12–14). Interactions between injected cells and the CAM microcirculation of living embryos were visualized, recorded, and quantified from the real-time video images. Cells were identified as intravascular (totally inside the microvasculature), in the process of extravasation (partially inside the microvasculature, with extravascular projections), or extravasated (completely outside of the microvessels). We established the proportions of fibroblasts in each of these positions at 3, 6, and 24 h p.i. We also studied the postextravasation migration of these cells through the mesenchyme tissue during the first 24 h p.i. by analyzing cell position relative to arterioles, venules, and lymphatics.

Statistical Analysis. Kruskal–Wallis one-way analysis of variance on ranks or Student's *t* test was used to statistically compare the analyzed populations, depending on whether the data distributions were normal or not and on the number of populations being compared. A level of $P < 0.05$ was regarded as statistically significant.

RESULTS

Intravital videomicroscopy allowed us to directly observe and compare cell interactions with the microvasculature (which proved to be similar for each of the three cell types) immediately following injection and at various times later. This made it possible to monitor cells from initial arrest (Fig. 1 *A* and *B*) right through to postextravasation migration within the mesenchyme (Fig. 1 *C* and *D*). Initial arrest always occurred by trapping of individual cells within microvessels on the basis of size restriction. All cells we observed entering the CAM microcirculation were trapped in this way, and none passed through the plexus to the venous outflow or attached to the walls of vessels larger than the cell diameter. Most of the cells were trapped in capillaries, but a few were first arrested within terminal arterioles (Fig. 1 *A* and *B*) and moved gradually from there into the capillaries. Cells lodged in the microvasculature blocked the blood flow at the site of arrest, and active cellular deformation and pseudopodial extensions were often observed within the vessel lumen, as the cells squeezed further into the capillary plexus. This cell deformation was required because the mean cell diameter before injection was 17 μm for all fibroblast types, whereas the mean capillary diameter is 9 μm (19). In summary, no differences in these processes of initial arrest and early interactions with the microvasculature were found among the three cell types. In no instance did we observe lysis of cells arrested within the microvasculature. Cells began to escape from the microcirculation (process of extravasation) within several hours of initial arrest.

Extravasation. Extravasation was observed exclusively from the capillary plexus, and cells of all three types always extravasated singly. The earliest event seen during this process was the formation of pseudopodia, which extended through the capillary wall into the mesenchyme layer. This was followed by

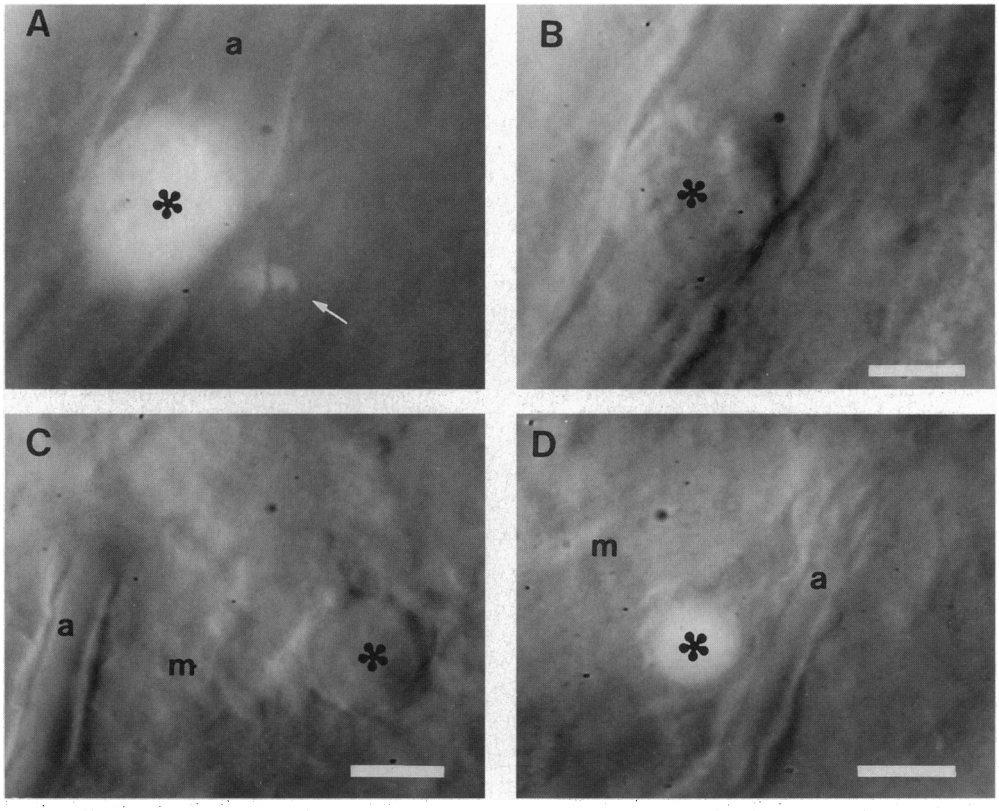

FIG. 1. Extravasation of fibroblasts viewed by intravital videomicroscopy. Cells fluorescently labeled with Calcein-AM are seen interacting with the microcirculation and the mesenchyme layer of chicken embryo CAM. Similar images were obtained from all three cell types. (*A*) Primary MEF (*) arrested at an arteriolar orifice leading to capillary plexus (which lies at a different plane of focus), seen by transillumination plus epifluorescence, 3 h p.i. Part of the cell remains within the arteriole (a) and part projects (→) into a capillary. (*B*) The same cell (*) shown by transillumination only. (*C*) MEF (*) extravasated from the capillary plexus, located in the mesenchyme (m) ≈40 μm distant from an arteriole (a) at 8 h p.i. Transillumination alone. (*D*) Extravasated MEF (*) observed at 6 h p.i., located in the mesenchyme (m) adjacent to a terminal arteriole (a). Transillumination plus epifluorescence. By focusing up and down with the microscope, long projections could be seen extending from the cell toward or over the abluminal surfaces of the arterioles in both *C* and *D*. These projections could be identified from the video monitor, but were seen even more clearly through the eyepieces. (Bars = 20 μm.)

transit of the cell body through the vessel wall. The extravasating cells had the appearance of sinking gradually from the plane of the plexus, allowing blood flow to resume progressively over top of them. No visible damage to the vessel wall was apparent during or after extravasation.

PAP2, NIH 3T3, and MEF cells extravasated equally well with the same timing of extravasation. By 3 h p.i., only ≈40% of the observed cells remained wholly intravascular (Fig. 2*A*). These numbers fell dramatically over the next 3 h, and, by 24 h p.i., virtually none of the cells remained intravascular (Fig. 2*A*). The mean percentages of cells in the process of extravasation fell from ≈40% to <10% between 3 and 24 h p.i. (Fig. 2*B*), with a concurrent increase in percentages of cells that had completed extravasation (Fig. 2*C*). By 24 h after injection, the mean percentages of PAP2, NIH 3T3, and MEF cells that had extravasated were 89%, 96%, and 96%, respectively (Fig. 2*C*). These values were not significantly different ($0.34 < P < 0.63$), indicating that the ability of these cell types to extravasate was independent of metastatic ability.

Migration Postextravasation. After extravasation, individual fibroblasts of all three cell types demonstrated, to the same degree, the ability to migrate within the mesenchymal layer. Extravasated fibroblasts were generally observed in the vicinity of arterioles (Fig. 1 *C* and *D*). In many cases, such cells exhibited multiple extensions encircling or spreading along the abluminal surfaces of the vessels. By focusing up and down with the microscope, these extensions could be seen very clearly, although they were not so obvious in views from a single plane of focus. Fig. 3 shows the mean percentages of observed cells that were in contact with or close to (within 1–20 μm) arterioles, venules, or lymphatics at 24 h p.i. The percentages of cells at any particular category of vessel were not significantly different for the three cell types ($0.32 < P < 0.83$; Kruskal–Wallis analysis). However, what was noteworthy was the marked preferential migration of fibroblasts of all three cell types to arterioles, rather than to venules or lymphatics ($0.001 < P < 0.004$; Student's *t* test).

DISCUSSION

Metastasis is known to be a complex multistep process, involving the interaction of many factors (including immune surveillance). Our focus in the present investigation was primarily on extravasation, which is thought to be a major rate-limiting step in metastasis. To study extravasation independently of host immune responses, we used an immune-deficient host, modeling the cancer cells that evade the immune system in the clinical situation. The chicken CAM provides a good model for studying extravasation. Although it is embryonic, its capillaries have a continuous endothelial lining and a complete basement membrane, exhibiting adult permeability properties at the time we injected the cells (12–14). It should be noted that the present study analyzes extravasation of intravenously injected cells from intact microvessels within the undamaged CAM, as opposed to invasion assays, which are performed by placing cells on the surface of the chorionic epithelium, using intact or wounded CAMs. We (22) and others (e.g., refs. 23 and 24) have shown that the integrity of the CAM is important for invasion studies, since wounded CAMs do not pose a barrier to invading cells.

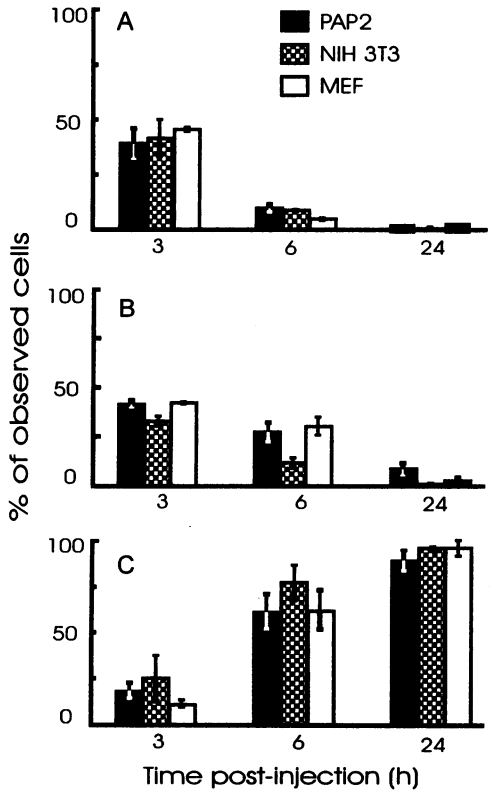

FIG. 2. Kinetics of extravasation of highly metastatic *ras*-transformed NIH 3T3 cells (PAP2), control nontransformed NIH 3T3 cells, and primary MEF cells from the CAM microcirculation. Percentages of cells which were intravascular (*A*), in process of extravasation (*B*), or had extravasated (*C*) are shown at 3, 6, and 24 h p.i. Different sets of experiments (involving different embryos) were performed at the stated time points. A total of 1481 cells were individually analyzed (average of 38 per experiment). Numbers of cells analyzed at 3, 6, and 24 h p.i., respectively, were as follows: PAP2, 124, 145, and 202; NIH 3T3, 123, 179, and 300; and MEF, 123, 163, and 122. The data showed no significant differences (Kruskal–Wallis one-way analysis on ranks) among the three cell types, at any of the stated time points, for cells which were intravascular (A, $0.48 < P < 0.99$), in process of extravasation (B, $0.28 < P < 0.68$), or extravasated (C, $0.34 < P < 0.63$). By 24 h p.i., >89% of observed cells of all three cell types had completed the process of extravasation. Bars represent means ± SE.

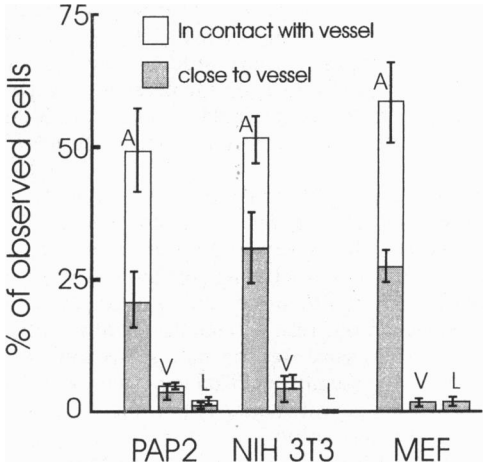

FIG. 3. Preferential migration of extravasated PAP2, NIH 3T3, and MEF cells to arterioles rather than venules or lymphatics. Stacked bar diagram showing percentages of observed cells that were in contact with (spreading around or along) and/or close to (within 1–20 μm) arterioles (A), venules (V), and lymphatics (L) at 24 h p.i. A total of 316 cells from 12 embryos was analyzed. Bars represent means ± SE. A marked preference for arterioles rather than venules or lymphatics was shown by all three cell types ($0.001 < P < 0.004$, Student's t test). No significant differences were found among the three cell types for any of the vessels ($0.32 < P < 0.83$, Kruskal–Wallis one-way analysis of variance on ranks).

We tested the hypothesis that the ability of cancer cells to extravasate is related to their metastatic potential. Contrary to current expectations, our results show that there was no difference in the ability of highly metastatic *ras*-transformed versus nontransformed but immortalized NIH 3T3 fibroblasts to extravasate from the microcirculation. In fact, nonimmortalized embryonic fibroblasts, which one would expect to exhibit little or no ability to extravasate, showed the same kinetics of extravasation as the other two cell types. Thus, we conclude that extravasation of *ras*-transformed versus control fibroblasts from the CAM microcirculation does not correlate with the metastatic ability or even transformed status of these cells.

It is noteworthy that the nontransformed (and nonmetastatic) cells not only extravasated but, thereafter, migrated through the mesenchymal layer to the same degree as the highly metastatic cells. In general, more metastatic cells are believed to be more invasive and motile than less metastatic cells (4, 25). *In vitro* studies have shown that PAP2 cells are more invasive than NIH 3T3 cells (17). Moreover, although embryonic fibroblasts exhibit high motility, perhaps reflecting their migratory role in embryonic morphogenesis, H-*ras*-transformed NIH 3T3 cells have been shown to be more motile *in vitro* than control NIH 3T3 cells (26). Therefore, we had expected the PAP2 cells to be more motile *in vivo* than NIH 3T3 cells. The fact that this was not the case shows that *in vitro* findings cannot always be extrapolated to the *in vivo* situation. It is interesting to note that primary MEF cells migrated after extravasation to the same degree as the other cell types analyzed. Our results show that for the cells and the model used in this study, postextravasation migration *in vivo* is not related to metastatic ability or transformed status of the cells.

This study shows quantitatively that after extravasation, the three types of fibroblasts all migrate preferentially to arterioles, rather than to venules or lymphatics, and encircle or spread over their abluminal surfaces. Since in a respiratory organ, such as the CAM, the O_2 saturation of blood is lower in arterioles than in venules, the cell migration toward arterioles cannot be explained on the basis of need for O_2. One might expect cells to migrate to regions rich in fibronectin, laminin, and collagen type IV (1, 3, 4, 25, 27). However, the distribution of these proteins appears to be the same in CAM arterioles and venules (28). Our studies with melanoma cells in the CAM have shown that they also migrate preferentially to arterioles and wrap around them (11, 19), indicating that this directed migration is not restricted to fibroblasts but is of more widespread significance. The reason for preferential binding to arterioles and the molecular basis of these events remain to be determined. Attachment of cells to various extracellular matrix components has been shown to confer protection from apoptosis (29), raising the possibility that attachment of extravasated cells to arterioles may in some way promote their survival. Periarteriolar locations are preferred sites of growth in the CAM for PAP2 cells (data not shown) and other metastatic cell lines (11, 20).

The steps in the metastatic process observed here are not unique to this model. The processes of initial arrest, extravasation, and migration exhibited by the three fibroblast cell types are similar in other cell lines we have studied: melanoma (9, 11, 19, 20, 30, 31) and mammary carcinoma (10). All the injected cells observed within the circulation were trapped by size restriction within microvessels at the inflow side of the microcirculation, and the cells withstood lysis by hemodynamic

forces. These same features are observed in chicken CAM (9–11, 19, 20), as well as in mouse liver (10, 30, 31) and muscle (30). For all cell types we have studied, the mechanism of extravasation in CAM and liver involves the escape of cells singly as opposed to intravascular replication followed by destruction of the vessel wall and extravasation of cells *en masse*.

Only a few of the cells that enter the circulation from a primary tumor successfully form metastases (32, 33). A number of mechanisms have been proposed to contribute to this metastatic inefficiency, including mechanical destruction of cells within the circulation and inability of cells to extravasate (3, 4, 32). However, our results from direct *in vivo* observation of cells during successive steps in metastasis show that major contributions to metastatic inefficiency may occur after extravasation. By means of a new experimental procedure to quantify the survival or loss of injected cells, we recently reported that >80% of all injected melanoma cells (two lines of different metastatic abilities) survived and successfully extravasated by 1 day p.i. in CAM (9). We also showed that the cell lines in that study did not differ in their rates of extravasation (11).

In summary, our study used intravital videomicroscopy to directly observe and quantify the ability of cells with very different *in vivo* and *in vitro* properties to extravasate from the chicken CAM microcirculation. The data demonstrate for the first time *in vivo* that highly metastatic *ras*-transformed PAP2 cells and nontransformed control cells (NIH 3T3, MEF) extravasate with the same kinetics from the CAM microcirculation. In addition, all three cell types show the same pattern of migration through the host tissue after extravasation. These results question the generally accepted dogma that metastatic potential is positively correlated with the ability of tumor cells to extravasate. Here we show that the ability to extravasate *in vivo* is not necessarily predictive of subsequent metastasis formation, pointing to postextravasation events as potential key determinants of metastatic ability.

We thank George Saab for technical assistance and Barbara Anderson for typing the manuscript. We are grateful to Drs. Christopher Ellis and Gregory Cairncross for reviewing the manuscript and for helpful comments. This work was supported by National Cancer Institute of Canada and Cancer Research Society Inc. S.K. is supported by a Scholarship from Fundação Coordenação de Aperfeiçoamento de Nível Superior, Brazil. A.F.C. is a Career Scientist of the Ontario Cancer Treatment and Research Foundation. R.K. is a Medical Research Council Scholar.

1. Liotta, L. A. (1986) *Cancer Res.* **46,** 1–7.
2. Goldfarb, R. H. & Brunson, K. W. (1989) in *Cancer Growth and Progression: Fundamental Aspects of Cancer*, ed. Goldfarb, R. H. (Kluwer Academic, Dordrecht, the Netherlands), Vol. 1, pp. 28–32.
3. Nicolson, G. L. (1991) *Curr. Opin. Oncol.* **3,** 75–92.
4. Stetler-Stevenson, W. G., Aznavoorian, S. & Liotta, L. A. (1993) *Annu. Rev. Cell Biol.* **9,** 541–573.
5. Weiss, L. (1990) *Adv. Cancer Res.* **54,** 159–211.
6. Liotta, L. A., Steeg, P. S. & Stetler-Stevenson, W. G. (1991) *Cell* **64,** 327–336.
7. Matrisian, L. M., Bowden, G. T., Krieg, P., Fürstenberger, G., Briand, J.-P., Leroy P. & Breathnach, R. (1986) *Proc. Natl. Acad. Sci. USA* **83,** 9413–9417.
8. Monsky, W. L. & Chen, W.-T. (1993) *Semin. Cancer Biol.* **4,** 251–258.
9. Koop, S., MacDonald, I. C., Luzzi, K., Schmidt, E. E., Morris, V. L., Grattan, M., Khokha, R., Chambers, A. F. & Groom, A. C. (1995) *Cancer Res.* **55,** 2520–2523.
10. Morris, V. L., Koop, S., MacDonald, I. C., Schmidt, E. E., Grattan, M., Percy, D., Chambers, A. F. & Groom, A. C. (1994) *Clin. Exp. Metastasis* **12,** 357–367.
11. Koop, S., Khokha, R., Schmidt, E. E., MacDonald, I. C., Morris, V. L., Chambers, A. F. & Groom, A. C. (1994) *Cancer Res.* **54,** 4791–4797.
12. Rizzo, V. & DeFouw, D. O. (1993) *Tissue Cell* **25,** 847–856.
13. Fitze-Gschwind, V. (1973) *Adv. Anat. Embryol. Cell Biol.* **47,** 1–51.
14. Chambers, A. F., MacDonald, I. C., Schmidt, E. E., Koop, S., Morris, V. L., Khokha, R. & Groom, A. C. (1995) *Cancer Metastasis Rev.* **14,** 279–301.
15. Hill, S. A., Wilson, S. & Chambers, A. F. (1988) *J. Natl. Cancer Inst.* **80,** 484–490.
16. Chambers, A. F., Denhardt, G. H. & Wilson, S. (1990) *Invasion Metastasis* **10,** 225–240.
17. Tuck, A. B., Wilson, S. M., Khokha, R. & Chambers, A. F. (1991) *J. Natl. Cancer Inst.* **83,** 485–491.
18. Bondy, G. P., Wilson, S. & Chambers, A. F. (1985) *Cancer Res.* **45,** 6005–6009.
19. MacDonald, I. C., Schmidt, E. E., Morris, V. L., Chambers, A. F. & Groom, A. C. (1992) *Microvasc. Res.* **44,** 185–199.
20. Chambers, A. F., Schmidt, E. E., MacDonald, I. C., Morris, V. L. & Groom, A. C. (1992) *J. Natl. Cancer Inst.* **84,** 797–803.
21. Lillie, F. R. (1965) *Development of the Chick: An Introduction to Embryology*, revised by Hamilton, H. L. (Holt, Rinehart & Winston, New York), pp. 267–291.
22. Chambers, A. F., Shafir, R. & Ling, V. (1982) *Cancer Res.* **42,** 4018–4025.
23. Ossowski, L. (1988) *J. Cell Biol.* **107,** 2437–2445.
24. Armstrong, P. B., Quigley, J. P. & Sidebotton, E. (1982) *Cancer Res.* **42,** 1826–1837.
25. Stracke, M. L., Aznavoorian, S. A., Beckner, M. E., Liotta, L. A. & Schiffmann, E. (1991) in *Cell Motility Factors*, ed. Goldberg I. D. (Birkhäuser, Basel), pp. 147–162.
26. Varani, J., Fligiel, S. E. G. & Wilson, B. (1986) *Invasion Metastasis* **6,** 335–346.
27. Nicolson, G. L. (1988) *Cancer Metastasis Rev.* **7,** 143–188.
28. Ausprunk, D. H., Dethlefsen, S. M. & Higgins, E. R. (1991) in *The Development of the Vascular System*, eds. Feinberg, R. N., Sherer, G. K. & Auerbach, R. (Karger, Basel), pp. 93–108.
29. Ruoslahti, E. & Reed, J. C. (1994) *Cell* **77,** 477–478.
30. Morris, V. L., MacDonald, I. C., Koop, S., Schmidt, E. E., Chambers, A. F. & Groom, A. C. (1993) *Clin. Exp. Metastasis* **11,** 377–390.
31. Morris, V. L., Schmidt, E. E., Koop, S., MacDonald, I. C., Grattan, M., Khokha, R., McLane, M. A., Niewiarowski, S., Chambers, A. F. & Groom, A. C. (1995) *Exp. Cell Res.* **219,** 571–578.
32. Liotta, L. A. & Stetler-Stevenson, W. G. (1991) *Cancer Res.* **51** (Suppl.), 5054s–5059s.
33. Schirrmacher, V. (1985) *Adv. Cancer Res.* **43,** 1–73.